Original article

Textile Research Journal

Textile Research Journal
0(00) 1–12

DOI: 10.1177/0040517512449066
trj.sagepub.com

SAGE

Influence of fiber diameter, fiber combinations and solid volume fraction on air filtration properties in nonwovens

Julien Payen[1,2], Philippe Vroman[1,2], Maryline Lewandowski[1,2], Anne Perwuelz[1,2], Sandrine Callé-Chazelet[3] and Dominique Thomas[3]

Abstract

In air filtration, nonwoven materials are known to be pertinent structures for fine filtration and moderate pressure drop. In order to develop a filter that combines good permeability and high efficiency, it is important to identify the relevant structural parameters of the nonwoven. The main criteria studied in this paper are fiber fineness, solid volume fraction and basis length (total length of fiber in unit area of nonwoven). The effect of combining different fiber diameters in order to reach the best compromise is also investigated. Our results show that the use of binary blends of different fiber diameters improves overall filtration behavior, in comparison to nonwoven filters with equivalent unimodal diameter distribution. A theoretical filtration model is used to predict filtration behavior for different structural characteristics and these predictions are compared to experimental results. However, this comparison demonstrates the limits of existing models in the case of fiber blends.

Keywords

aerosol filtration, fibrous filter, fiber blends, spunlaced nonwovens

Nonwoven filter media are widely used in liquid and gas filtration.[1] In Europe, in 2007, 98,300 tons of nonwovens were used in filtration, around 40% of which were for aerosol filtration. Nonwovens are potentially better filters than woven fabrics: they are cheaper to produce, are versatile and offer a wide range of functionalities, especially in the range of sub-micron aerosols. In these materials, fiber fineness can vary from micrometer to millimeter range, fabric thickness from micrometer to centimeter range and basis weight can range from 1 to 2000 g/m^2.[2]

Within the nonwoven structure, the characteristics of the fibers assume a dominant role on the filtration performance, namely through their geometrical properties. Different papers have dealt with this issue, some of which are recalled here. The first parameter is fiber fineness: decreasing fiber diameter increases filtration efficiency, due to the increased impact probability resulting from a greater number of fibers.[3–5] Increasing fiber surface roughness is found to improve the collection efficiency of nanoparticles due to the presence of asperities,[6] whereas the use of special fiber cross-section shape, for example multilobal, leads to an increase in specific surface area, and hence to improved collection efficiency.[6–8] Another fiber characteristic, fiber crimp, is also found to enhance both efficiency and pressure drop characteristics.[6,7]

The structural characteristics of the nonwoven filter are also of paramount importance: for instance, increasing the solid volume fraction (SVF, also called packing density or compacity) will generally increase both filtration efficiency and pressure drop.[9,10] The use of fiber blends can also improve filter properties

[1]Univ Lille Nord de France, France
[2]ENSAIT, GEMTEX, France
[3]Université de Lorraine/LRGC/CNRS, France

Corresponding author:
Philippe Vroman, ENSAIT, 2 allée Louise et Victor Champier, 59056 Roubaix Cedex 1, France
Email: philippe.vroman@ensait.fr

by increasing the filtration depth and creating three dimensional structures.[11,12] In specific studies on needlepunched nonwovens, Krucinska[13] and Zobel et al.[14] showed that process parameters, such as gauge or penetration depth of needles, also influenced the filtration properties.

In addition to filter characteristics, the nature of aerosol will also have an effect on particle collection. Raynor and Leith,[15] Contal et al.[16] and Thomas et al.[17] observed a lower filtration efficiency with liquid aerosols when compared to solid aerosols.

Decreasing indefinitely the fiber diameter to improve filtration efficiency is not possible, since pressure drop will become unacceptable. The use of electret filters is one way to overcome this problem:[18–20] numerous filter media are electrostatically charged. This treatment is usually performed during or after the production of the nonwoven filter media. However, the permanency of this treatment is not completely guaranteed, since it can be for example deteriorated by solvents.[18,21,22] Electret filters can be found in respirators, for example, where the media is often a spunbond/meltblown combination. One of the drawbacks is the life span of these respirators: clogging occurs after a few hours, making it difficult to breathe through them.

Another idea to enhance filtration performance is to vary the SVF of the nonwoven, or to use blends of different fiber diameters, and this will be the chosen course of action in our work. Our purpose is to understand the filtration mechanism through a study of the influence of fiber diameter, fiber blends and SVF on filtration properties of spunlaced nonwovens. The use of models to predict filtration behavior over a wide aerosol range will be investigated and will also be presented in comparison with our experimental results.

Filtration theory in fibrous structures

An aerosol is a fine suspension in air of liquid or solid particles that are small enough to be stable, with a size usually below 100 µm. The first stage for solving all problems entailed by aerosol particle filtration consists of a good description of the flow fields around fibers inside the filter. Generally, filters are schematically depicted as a structure of "cells", each cell corresponding to a fiber roughly described by a cylinder surrounded by the fluid.

The Kuwabara cell model is the most used[23] and shows the importance of the SVF (denoted by α in mathematical formula). It is defined by the following expressions:

$$H_{ku} = \alpha - 0.5 \times \ln(\alpha) - 0.25 \times \alpha^2 - 0.75 \quad (1)$$

$$\alpha = 10 \times \frac{G}{\rho_f \times Z} \quad (2)$$

where H_{ku} is a hydrodynamic factor, G is the basis weight (mass per unit area, g/m^2), ρ_f is the fiber material density (g/cm^3) and Z is the filter thickness (mm).

Lee and Liu[24] and Davies[25] present various mechanisms of particle capture according to particle size and electric charges to model filtration efficiency of a fibrous filter.

When electrostatic forces can be neglected, the main mechanisms are Brownian diffusion (η_d), direct interception (η_r) and inertial impaction (η_i) (see Figure 1).

The first mechanism occurs with small particle sizes (<0.1 µm). The particles are subjected to thermal agitation around the air streamlines and are collected by the fibers. The capture by Brownian diffusion is formulated by the Péclet number Pe:

$$Pe = \frac{U_f \times d_f}{D} \quad (3)$$

where d_f is fiber diameter, U_f is flow velocity and D is the diffusion coefficient defined by Equation (4):

$$D = \frac{k_B \times T \times Cu}{3 \times \pi \times \mu \times d_p} \quad (4)$$

where T and μ are, respectively, the air temperature and the viscosity, k_B is the Boltzmann constant and d_p is the particle diameter. Cu is the Cunningham coefficient related to the particle diameter and air molecule free path given by Equations (5) and (6):

$$Cu = 1 + Kn_p\left(A + B \times \exp\left(-\frac{C}{Kn_p}\right)\right) \quad (5)$$

$$Kn_p = 2\frac{\lambda}{d_p} \quad (6)$$

where A, B and C are Cunningham coefficient factors. Kn_p is called the Knudsen number of particles and is

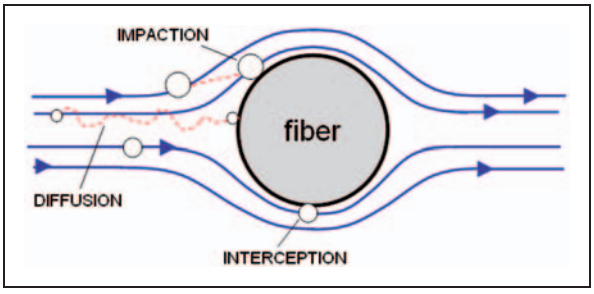

Figure 1. Aerosol capture mechanisms.

related to the particle diameter and air molecule mean free path λ.

The second mechanism occurs when the distance between the center of the particle and the fiber is less than the particle radius. It is effective for moderate particle sizes (>0.1 μm). The particle is intercepted by the fiber, and the interception ratio, R, is given by the following equation:

$$R = \frac{d_p}{d_f} \tag{7}$$

This factor gives an indication of the probability of collecting particles through interception.

The third mechanism is effective for greater particle sizes (>1 μm), which are not able to follow air stream lines due to their inertia, and so they are impacted on the fibers. Inertial impaction is governed by Stokes number St:

$$St = \frac{U_f \times d_p \times \rho_p}{18 \times \mu \times d_f} \tag{8}$$

where ρ_p is the density of the particle.

All these collection mechanisms show the relative importance of fiber diameter.

Most authors[26] assume that the efficiency of the individual fiber is the sum of the corresponding efficiency capture mechanisms:

$$\eta = \sum \eta_j \tag{9}$$

Different authors – Miecret, Gustavsson, Lee, Liu, Rubow, Payet, Gougeon, Stechkina et al., Kirsch et al. – have proposed different models to calculate η_d, η_r and η_I,[27] which are, respectively, single fiber efficiency towards diffusion, interception and inertia.

The clean filter removal efficiency E is closely related to the single fiber collection efficiency η according to an expression obtained by operating a mass balance on a filter element of thickness dz and integrated on the total filter thickness Z:

$$E = 1 - \exp\left(-\frac{4 \times \alpha \times \eta \times Z}{\pi(1-\alpha) \times d_f}\right) = 1 - \exp(-\Phi \times Z) \tag{10}$$

For particle sizes between 0.1 and 1 μm, the usual particle capture mechanisms – direct interception, inertial impaction and diffusion – become less effective and lead to greater aerosol penetration. This is characterized by the Most Penetrating Particles Size (MPPS).

Materials and experimental details

Nonwoven filter structures

Nonwoven samples were produced using pilot lines. They were obtained by carding, lapping, pre-needling and spunlacing processes. The spunlacing process, or hydroentanglement, uses high-speed water jets to impinge the fiber web so that the fibers intertwine around each other and provide cohesion to the web. In our study, the spunlacing process was based on two manifolds: the first one was set at 95 bars and the second one at 175 bars, working on both sides of the nonwoven.

The web was then dried in an oven at 160°C, and in order to adjust the SVF, the web was also compacted at a moderate temperature, below the glass transition temperature of the fibers.

A series of polyester (PET, poly ethylene terephtalate) fibers, with linear densities varying from 0.9 to 17 dtex (supplier data), have been used. Table 1 gives their average diameters measured from scanning electron microscope (SEM) images of the nonwovens, determined from 300 diameter measurements for each material with the help of image processing software (ImageJ). The diameters obtained ranged from 10.9 to 45.1 μm. Some differences between supplier data and linear densities calculated from experimental diameters can be observed.

Two series of nonwovens are manufactured: the first one is based on only one diameter type, called unimodal fiber diameter (UFD) distribution nonwovens, while the second series is obtained with fiber blends of two different fiber diameters, called bimodal fiber diameter (BFD) distribution nonwovens.

The structural characteristics of the series of UFD nonwovens produced are presented in Table 2. They are listed in decreasing order of fiber diameter. Their names (Table 1) are related to the fiber diameter and to the basis weight. The SVF is calculated with Equation (2). Standard deviations for all characteristics showed that the samples were quite homogeneous.

Three basis weights (150, 200 and 300 g/m^2) have been targeted, after pre-needling. The final basis weights were, however, different from these values for processing reasons.

The fiber basis length (km/m^2) represents the total length of fiber per unit surface area, and is thus obtained by the following relation:

$$L = \frac{G}{T_f} \times 10 \tag{11}$$

where L is the basis length in km/m^2, G is the basis weight in g/m^2 and T_f is the fiber linear density in

dTex. In the case of blends, the basis length of one of the constituent fibers can be calculated with the same equation by considering the weight of this fiber in the blend.

A decrease in fiber diameter increases the total basis length of fibers as there are more fibers for a given basis weight. This means that there are also more fibers for a given area.

For a given basis weight, the thickness is greatly reduced with the use of finer fibers. Decreasing fiber diameter tends to increase the SVF. This is probably related to the entangling effect of the spunlacing operation, which is more efficient with finer fibers.

The second series of nonwovens, BFD distributions, are produced with binary fiber blends. The coarsest fiber L, 45.1 μm, is introduced for this series. The finest fiber E, 10.9 μm, is used in all blends, either in combination with fiber A (28.2 μm) or fiber L.

Table 1. List of fiber diameters used

Fiber	Linear density supplier data (dtex)	Diameter[a] (μm)	Calculated linear density[b] (dtex)
A	6.7	28.2 ± 2.3	8.61 ± 0.06
B	5	23.6 ± 2.1	6.03 ± 0.05
C	3.3	16.5 ± 1.4	2.95 ± 0.02
D	1.5	11.5 ± 1.2	1.43 ± 0.02
E	0.9	10.9 ± 0.7	1.29 ± 0.01
L	17	45.1 ± 3.4	22 ± 0.13

[a]Measured experimentally. [b]Calculated from measured diameter.

The proportions of the fibers have been calculated so as to obtain the final nonwovens with an equivalent average fiber fineness corresponding to two reference nonwovens, C2 (16.5 μm) or D2 (11.5 μm). T_f, the targeted average linear density in dTex, is determined from the following equation:

$$\frac{1}{\left(\frac{m_1\%}{T_1}\right)+\left(\frac{m_2\%}{T_2}\right)} = T_f \qquad (12)$$

T_1 and T_2 are, respectively, the linear densities of fibers 1 and 2, while $m_1\%$ and $m_2\%$ are their mass fractions. The calculated mass fractions for each blend are given in Table 3, along with the characteristics of the blends and their reference UFD nonwovens. The numerical fractions have also been calculated and are presented in Table 3, as they will be used in the filtration models.

The LE (10.9/45.1 μm) fiber blends led to thicker and more porous nonwovens than the AE (10.9/28.2 μm) blends. This was probably due to the presence of the coarse 45.1 μm fibers, which tend to open up the structure. Figure 2 shows SEM images of AE(D2) and LE(D2) samples. The blends are intimate and, with regard to basis length of fine fibers (Table 3), the LE sample has more finer fibers in proportion than the AE sample, and this is quite visible on the microphotographs.

Test methods

The filtration properties of the nonwovens were evaluated by measuring their filtration efficiency in the

Table 2. Structural characteristics of unimodal fiber diameter distribution nonwovens

Non woven	Targeted basis weight (g/m^2)	Fiber diameter d_f (μm)	Final basis weight G (g/m^2)	Thickness Z (μm)	SVF (%)	Basis length L (km/m^2)
A2	200	28.2 ± 2.3	216 ± 8	986 ± 21	15.9 ± 0.5	250
B2	200	23.6 ± 2.1	220 ± 6	1050 ± 20	15.2 ± 0.2	364
C1	150	16.5 ± 1.4	141 ± 4	600 ± 20	17.0 ± 0.4	478
C2	200	16.5 ± 1.4	215 ± 8	884 ± 23	17.7 ± 0.8	728
C3	300	16.5 ± 1.4	317 ± 12	1280 ± 30	17.9 ± 0.4	1074
D1	150	11.5 ± 1.2	134 ± 6	500 ± 10	19.4 ± 0.4	934
D2	200	11.5 ± 1.2	210 ± 8	780 ± 32	19.5 ± 0.8	1468
D3	300	11.5 ± 1.2	314 ± 11	1090 ± 40	20.9 ± 0.8	2189
E1	150	10.9 ± 0.7	131 ± 4	510 ± 10	18.6 ± 0.5	1017
E2	200	10.9 ± 0.7	207 ± 7	776 ± 21	19.4 ± 0.4	1606
E3	300	10.9 ± 0.7	309 ± 10	1050 ± 30	21.3 ± 0.6	2398

SVF: solid volume fraction.

Table 3. Fiber composition and characteristics of binary fiber blends

	Fiber composition			Mean binary diameter	Basis weight	Thickness	SVF	Basis length L (km/m^2)	
Nonwoven	Fiber diameter	Mass fraction	Numerical fraction	d_f (μm)	G (g/m^2)	Z (μm)	(%)	Fine fiber	Coarse fiber
C2	16.5 μm	100%	100%	16.5 μm	215 ± 8	884 ± 23	17.7 ± 0.8	728	
AE(C2)	10.9 μm	15%	57%	16.5 μm	246 ± 9	776 ± 27	17.0 ± 0.6	410	
	28.2 μm	85%	43%						312
LE(C2)	10.9 μm	23%	85%	16.5 μm	214 ± 3	884 ± 52	11.6 ± 0.3	548	
	45.1 μm	77%	15%						97
D2	11.5 μm	100%	100%	11.5 μm	210 ± 8	780 ± 32	19.5 ± 0.8	1468	
AE(D2)	10.9 μm	55%	90%	11.5 μm	228 ± 6	960 ± 27	17.2 ± 0.6	1394	
	28.2 μm	45%	10%						154
LE(D2)	10.9 μm	58%	96%	11.5 μm	224 ± 5	1070 ± 18	15.2 ± 0.5	1443	
	45.1 μm	42%	4%						56

SVF: solid volume fraction.

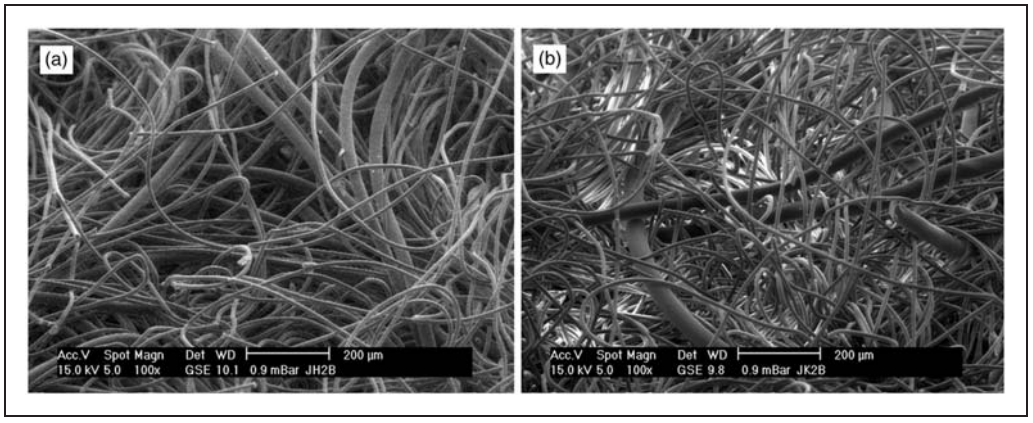

Figure 2. Scanning electron microscope images of two blended nonwovens. (a) AE(D2): 10.9/28.2 μm blend. (b) LE(D2): 10.9/45.1 μm blend.

MPPS region. A solid aerosol obtained from a soda fluorescein solution is used. The experimental set-up consisted of an aerosol generator, a vertical filter holder (95 cm^2) and the control device of the filtration volume flow rate. Two aerosol sampling lines upstream and downstream of the filter allowed the measurement of the aerosol size distribution by an ELPI (Electric Low Pressure Impactor). The particle size distribution was found to be log normal with a mean diameter of 0.18 μm. Flow velocity was set at 4 cm/s and the test duration at 3 min. The complete description of this method can be found in Thomas et al.[26] The filtration efficiency is determined by measuring the amount of aerosol particles on the test filter and on the absolute filter placed after the test filter to collect all the particles that were not stopped.

Filtration efficiency depends on the thickness of the sample and, to compare nonwovens with different thicknesses, a specific efficiency expressed per unit thickness is calculated, assuming that the filter structure is homogeneous throughout its thickness. Considering Equation (10), this standard value of E for a 1 mm thick sample, noted E^*, can be calculated by the following equation:

$$E^* = 1 - \exp\left(\frac{\ln(1-E)}{Z}\right) \tag{13}$$

E is the efficiency measured experimentally for the filter sample of thickness Z. The MPPS region for our structures has been found to be between 0.1 and 3 μm.

The air permeability of all nonwovens is measured according to the test standard ISO 9237 using a Textest FX 3300 instrument at a fixed pressure drop of 200 Pa. This parameter also depends on the material thickness and, for a laminar air flow, the air permeability is a linear function of thickness. The air permeability can thus be calculated for a unit thickness by simply dividing the experimental air permeability by the thickness value in mm. The conditions for laminar air flow have been verified for all samples, except for A2, B2 and C3, by calculating the limit flow velocity U_0 for a Reynolds number: $(Re = \rho U_0/S_p) < 1$. Some precaution is therefore needed when analyzing the results of these samples. For A2 and B2, the reason can be attributed to their higher air permeability, since these samples have the lowest SVF: a higher air flux will favor a turbulent regime. For sample C3, the reason is not clear.

In filtration, the Quality Factor, QF, is sometimes used to compare qualitatively and quantitatively different filters:[27]

$$QF = \frac{-\ln(1-E)}{\Delta P} \tag{14}$$

Table 4. Filtration properties of unimodal fiber diameter distribution nonwovens

Nonwoven	E^* (%)	Air permeability* ($l\,s^{-1}\,m^{-2}$)
A2	12.50 ± 0.14	1691 ± 77
B2	28.41 ± 3.54	1499 ± 107
C1	28.60 ± 4.24	779 ± 81
C2	45.39 ± 5.08	662 ± 32
C3	56.29 ± 3.67	663 ± 34
D1	66.65 ± 2.01	264 ± 28
D2	70.99 ± 6.42	257 ± 19
D3	73.76 ± 2.88	194 ± 7
E1	70.15 ± 9.49	185 ± 17
E2	83.09 ± 2.13	172 ± 3
E3	83.97 ± 1.26	131 ± 8

*for unit thickness of 1 mm.

Results and discussion

Unimodal fiber diameter distribution nonwovens: influence of fiber diameter and SVF

The filtration efficiency and air permeability of all the UFD samples are presented in Table 4. The efficiency values cover a wide range, from 12.5 to 84%, increasing rapidly when the fiber diameter decreases from 28 to 11 μm. On the other hand, air permeability falls from 1691 to 1311 $s^{-1}\,m^{-2}$ over this fiber diameter range.

These results are expressed graphically in Figures 3–5. Figure 3 shows filtration efficiency as a function of air permeability for all investigated samples: an inversely proportional relationship is found between these two properties, as expected.[25] It can also be observed that efficiency increases as fiber diameter decreases, which is also expected.

Figure 4 shows that, in general, filtration efficiency increases logarithmically with the basis length of fibers, whatever the SVF of the tested sample, which ranges from 15 to 21%. This limited effect of packing density on filtration efficiency is in agreement with the work of Lamb and Costanza,[3] which showed that for a SVF below 10%, filtration efficiency tends to decrease as

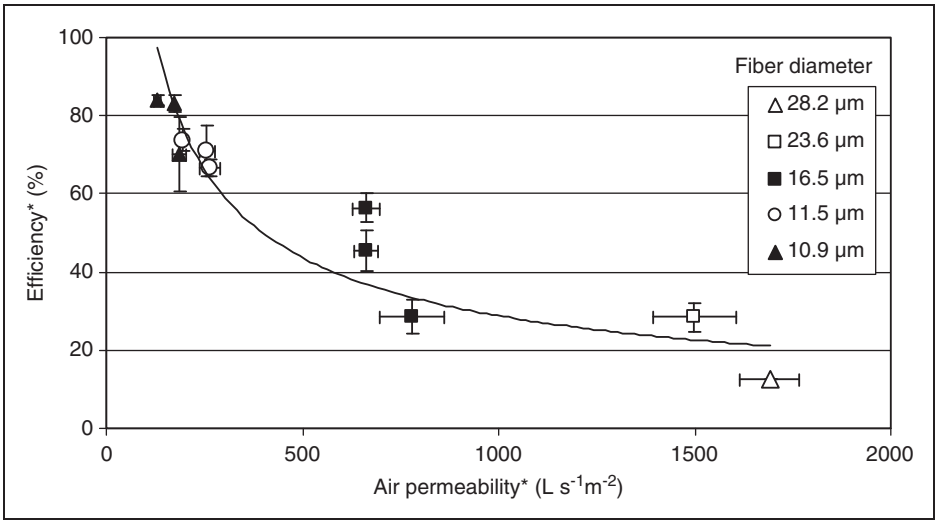

Figure 3. Filtration efficiency E^* versus air permeability* for unimodal fiber diameter (UFD) nonwovens.

SVF decreases, but also found no clear dependence of efficiency on SVF in the range of our study (15–21%).

The graph of efficiency plotted against SVF (Figure 5) indeed shows that although there seems to a general tendency for efficiency to increase with nonwoven compacity, for a given compacity (19.4%, for example), different values of efficiency can be obtained. This means that filtration performance is not solely based on this parameter, but also on the fiber or pore organization inside the structure.

Various existing filtration models, reviewed in the first section, have been tested with our experimental results. The best fitting model was found to be the "LRG" model.[28] This model is in fact composed of contributions from Liu and Rubow[29] and Gougeon.[30] The single fiber efficiencies corresponding to the different particle capture mechanisms, described previously in the theoretical part, are defined by the following equations for this model:

$$\eta_d = 1.6 \times \left(\frac{1-\alpha}{H_{ku}}\right) \times Pe^{-2/3} \times Cd \tag{15}$$

with

$$Cd = 1 + 0.388 \times Kn_f \times \left(\frac{(1-\alpha) \times Pe}{H_{ku}}\right)^{1/3} \tag{16}$$

$$\eta_r = 0.6 \times \frac{1-\alpha}{H_{ku}} \times \frac{R^2}{1+R} \times Cr \tag{17}$$

with

$$Cr = 1 + 1.996 \times \frac{Kn_f}{R} \tag{18}$$

$$\eta_i = 0.0334 \times St^{3/2} \tag{19}$$

This model depends on four material structural parameters – fiber density, basis weight, thickness, mean fiber diameter – and a fifth factor, which is fluid velocity.

The model can be further simplified to yield the following equations, which show clearly their dependency on d_f and α (SVF calculated from fiber density, basis weight and thickness, Equation (2)):

$$\eta_d = \frac{k_3 f(\alpha)}{d_f^{2/3}\left(1 + k_4 \frac{f(\alpha)}{d_f^2}\right)^{1/3}} \tag{20}$$

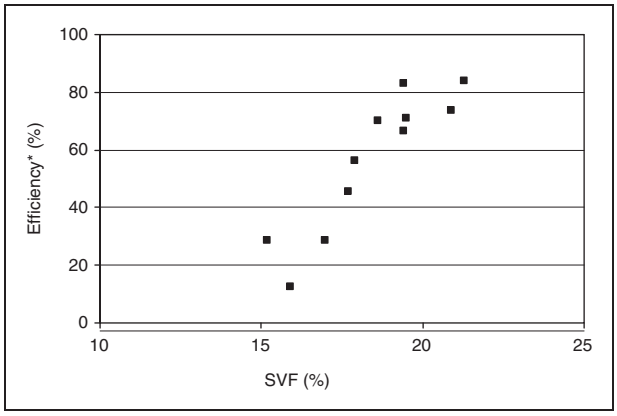

Figure 5. Filtration efficiency E^* versus solid volume fraction (SVF).

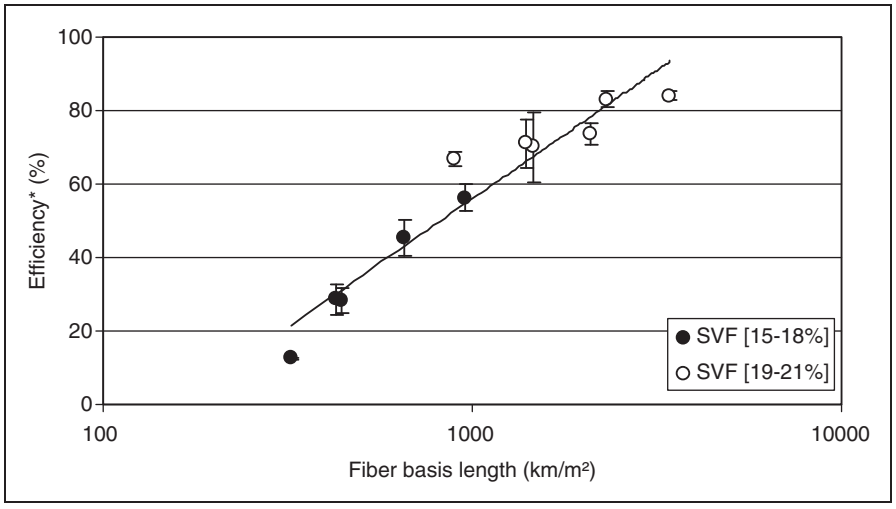

Figure 4. Filtration efficiency E^* versus fiber basis length.

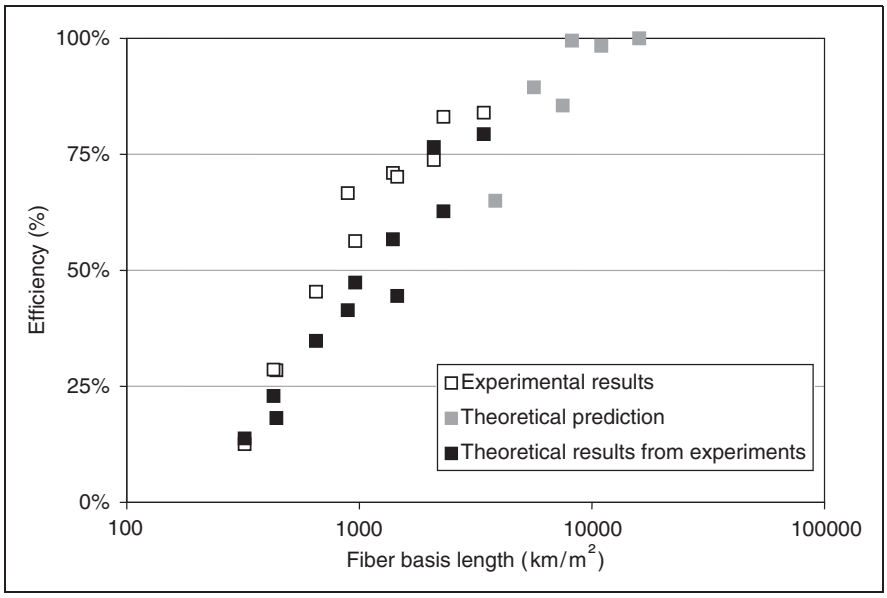

Figure 6. Comparison of experimental efficiency and predicted efficiency with the Liu, Rubow and Gougeon model (LRG) model.

Table 5. Filtration properties of bimodal fiber diameter nonwoven samples

Nonwoven	E^* (%)	Air permeability* ($l\,s^{-1}\,m^{-2}$)	Quality Factor ($\times 1000$) QF (Pa^{-1})
C2	45.39 ± 5.15	662 ± 46	1.93
AE(C2)	30.78 ± 2.18	976 ± 60	2.69
LE(C2)	46.26 ± 2.18	2087 ± 129	12.68
D2	70.99 ± 1.66	257 ± 9	2.55
AE(D2)	58.83 ± 9.18	347 ± 32	1.23
LE(D2)	71.50 ± 1.14	560 ± 36	4.94

$$\eta_r = \frac{k_2 f(\alpha)}{d_f^2} \tag{21}$$

$$\eta_i = \frac{k_1}{d_f^{3/2}} \tag{22}$$

where $f(\alpha) = \frac{1-\alpha}{H_{ku}}$, and k_1, k_2, k_3 and k_4 are constants.

Figure 6 shows the experimental efficiency (open symbols) and the theoretical values obtained with the LRG model (black symbols for comparison with experiments, gray symbols for prediction).

There seems to be a relatively good agreement between experimental and theoretical results, and the fiber basis length proves to be an interesting parameter to consider when designing filter media with unimodal diameter distribution.

Nonwovens with bimodal fiber diameter distribution: influence of fiber diameter blends

The results obtained with the nonwovens produced from fiber blends are given in Table 5. The results corresponding to the reference UFD samples are also presented. Standard deviations show a good homogeneity in all samples except AE(D2) for filtration efficiency.

Figure 7 shows the air permeability results, along with the SVF, of the nonwovens. Filter media containing fiber A (28.2 μm) are more compact compared to those containing fiber L (45.1 μm), which explains the much lower air permeability measured for the A blends.

The air permeability of the BFD nonwovens is much higher than that of the UFD sample, even more so for the L blends: this is a consequence of the decrease in SVF.

Regarding filtration efficiency results (Figure 8), the A blends are less efficient than their respective references C2 and D2. On the other hand, the L blends are more efficient than their UFD counterparts, with a smaller SVF but a greater fiber basis length.

If we consider the QF (Equation (14)), also represented in Figure 8, the L blends containing the coarsest fiber L show a much better filtration performance than the finer fiber blends and than the unimodal fiber nonwovens. This is especially visible on the nonwovens with the average fiber diameter of 16.5 μm.

These results may be due to the fact that the mass fraction of the finest fiber, E (10.9 μm), is more

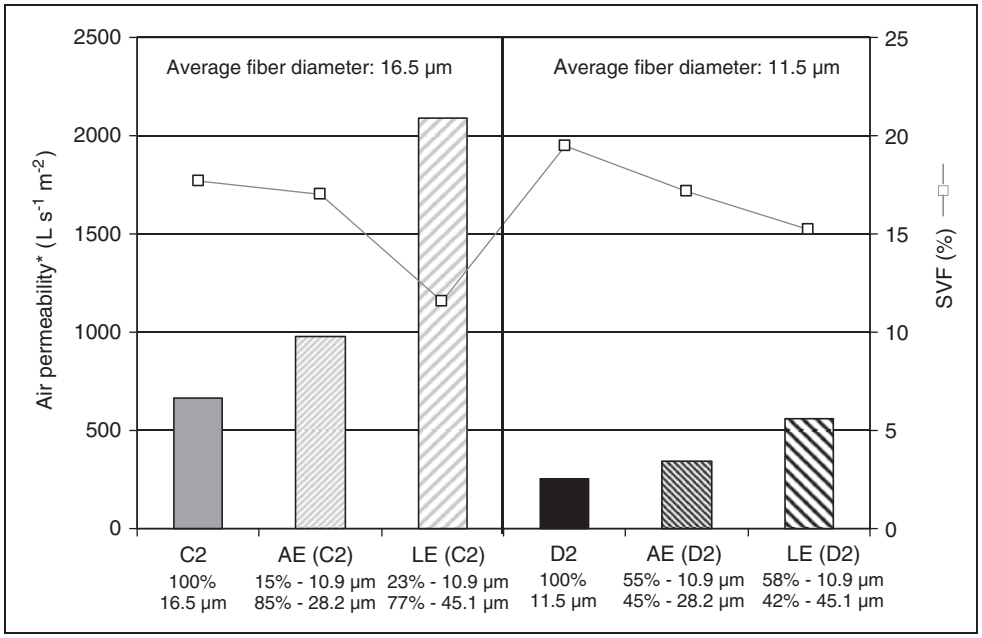

Figure 7. Air permeability and solid volume fraction (SVF) of nonwoven blends and reference samples.

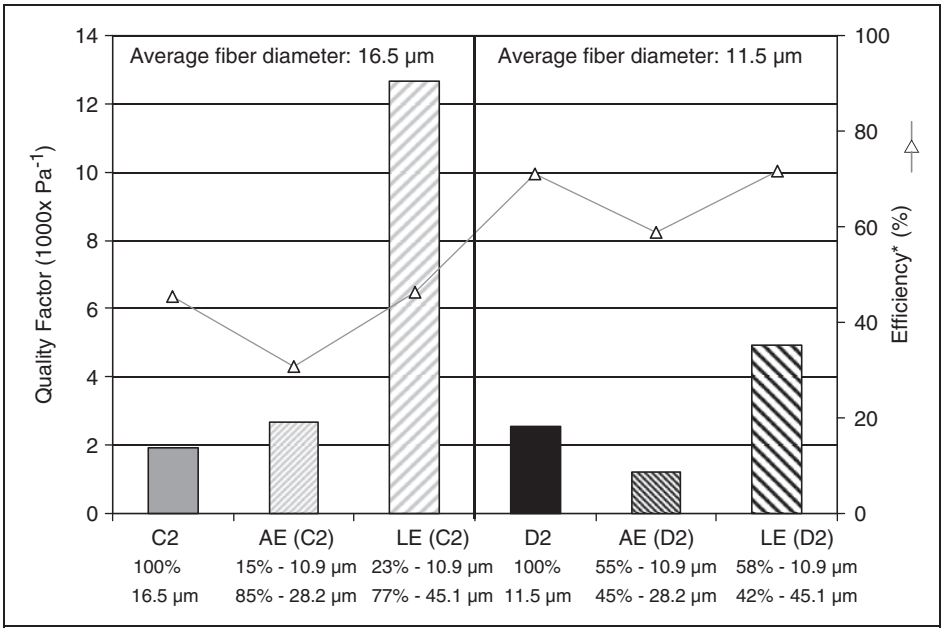

Figure 8. Quality Factor and specific filtration efficiency of nonwoven blends and reference samples.

important in the L blends, but also because structure configuration, such as pore size distribution and fiber arrangement, is particularly optimized and favors filtration efficiency and air permeability. Similar results have been obtained in another property concerning liquid absorption: the presence of two fiber diameters lead to a narrower pore size distribution compared to structures containing only one fiber diameter, and favored liquid retention behavior.[31]

Indeed, if the filtration efficiency is plotted against the fine fiber's total length per unit area (Figure 9), a linear-type relationship is obtained. This result is in agreement with the work of Sakano et al.,[32] which shows that the filtration efficiency is proportional to the mass fraction of fine or coarse fibers. Considering that the samples have similar basis weights, the total basis length is indeed proportional to the mass fraction of one constituting fiber.

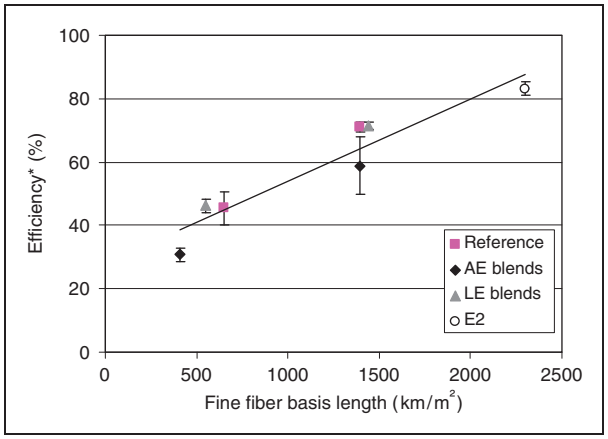

Figure 9. Filtration efficiency E^* versus fine-fiber basis length.

Table 6. Experimental and theoretical filtration efficiencies for bimodal fiber diameter nonwoven blends

		Liu, Rubow and Gougeon model (LRG) model		
Nonwoven	Experimental (%)	Average diameter approach (%)	Sakano's approach mass fraction (%)	Numerical fraction approach (%)
C2	41.44%	32.34%		
AE(C2)	32.04%	26.42%	24.07%	35.47%
LE(C2)	56.48%	17.52%	14.11%	35.63%
D2	61.92%	55.29%		
AE(D2)	57.52%	49.92%	28.20%	61.66%
LE(D2)	73.77%	39.98%	34.94%	47.42%

As a conclusion, it seems that filtration efficiency is mainly controlled by the number of fine fibers present in the media: a minimum amount is required to ensure a certain level of filtration efficiency. The presence of coarser fibers will influence the air permeability of the media, by opening up the structure and decreasing the SVF. Fiber arrangement and different pore configurations may affect and increase both efficiency and air permeability.

Sakano et al.[32] propose a model that is the first to take into account a filter composed of two different fiber diameters. They give the following expression for filtration efficiency in a bimodal fiber fineness distribution filter:

$$E = 1 - \exp\left[-\frac{4 \times \alpha \times Z}{\pi(1-\alpha)}\left(\frac{m_1\eta_1}{d_{f1}} + \frac{m_2\eta_2}{d_{f2}}\right)\right] \quad (23)$$

where df_1 and df_2 are, respectively, the fine and coarse fiber diameters, m_1 and m_2 are their mass fractions and η_1 and η_2 are their initial efficiencies. This expression is obtained from Equation (10) by replacing the fiber diameter parameter df by a parameter that takes into account the blend of two fiber diameters. This results from the direct application of linearity between mass fraction of fibers and filtration efficiency proposed by Sakano et al.:[32]

$$\frac{\eta}{d_f} = \frac{m_1\eta_1}{d_{f1}} + \frac{m_2\eta_2}{d_{f2}} \quad (24)$$

Another possibility would be to take into account the numerical fraction, n_i, instead of the mass fraction:

$$\frac{\eta}{d_f} = \frac{n_1\eta_1}{d_{f1}} + \frac{n_2\eta_2}{d_{f2}} \quad (25)$$

We have calculated the filtration efficiency of the blends using the LRG model, but we have compared the use of the Sakano approach for the fiber diameter (Equation (24)) to the usual average fiber diameter calculation. The calculation of efficiency was also done using the numerical fraction values of the blends given in Table 3 and using Equation (25). The experimental and theoretical filtration efficiencies, for a thickness of 1 mm and mean particle size of 0.18 μm, are presented in Table 6.

There is not a good agreement between experimental results and either model. The linearity observed in experimental results and described in the work of Sakano et al.[32] is not confirmed here. The numerical fraction approach seems to give better results, especially for the AE blends, but the agreement is far from satisfactory.

This tends to prove that some of the structural characteristics, such as fiber arrangement, tortuosity, heterogeneity and so on, which are not taken into account in existing models, are significant for complex fibrous structures. Besides, we cannot consider the two coexisting fiber populations as independent in terms of their contribution to filtration efficiency, as supposed by the theoretical models. This example demonstrates the limitations of existing models and encourages modeling of other important nonwoven structural characteristics. Recent works concerning modeling of pressure drop and initial filtration efficiency that make use of fiber size distributions result in better agreement with experiments.[33–35]

Conclusion

We have developed nonwoven structures with some specific and controlled characteristics with the aim of

obtaining nonwoven air filters that will combine good filtration efficiency and acceptable permeability. We have focused our study on the influence of fiber fineness, fiber blends and SVF.

Our results show that, for UFD samples, in addition to confirming that decreasing fiber diameter improves filtration efficiency to the detriment of air permeability, the SVF seems to have a limited effect on the range we used (from 15 to 21%).

Interesting results have been obtained with BFD blends. The combination of coarse and fine fibers improved nonwoven filtration behavior compared to the equivalent unimodal diameter samples, especially when there is a great difference between the two fiber diameters in the blend. The use of the fiber basis length to analyze our results shows that the key parameter to a good efficiency is the basis length of fine fiber present in the structure. Adding very coarse fibers to a fine-fiber filter opens up the structure, and leads to a more efficient spatial organization of the fibers, decreasing the SVF and allowing a better passage of air.

Finally, we applied existing filtration models to our experimental results: we found a very good agreement of the unimodal diameter nonwovens with the LRG model. On the other hand, the results of our binary blends could not fit with existing models, even if the consideration of the numerical fraction instead of the mass fraction improves the results. Further work need to be done to take into consideration more complex fiber diameter distributions in these models.

Acknowledgement

We would like to acknowledge Philippe Van Coetsem and Michel Caucheteux from IFTH (Institut Français Textile Habillement) for their technical support concerning nonwoven manufacture and Béatrice Castel from Institut Français Textile-Habillement (IFTH) for her contribution concerning SEM acquisition.

Funding

This work was supported financially by the ''FEDER'' and the ''Nord-Pas-de-Calais'' Region.

References

1. Sutherland K. *Profile of the international filtration & separation industry: Market prospects to 2009*. Oxford: Elsevier, 2005.
2. Gregor E. Primer on nonwoven fabric filtration media, http://www.egregor.com (2003), Accessed: February 2011.
3. Lamb G and Costanza PA. Influences of fiber geometry on the performance of nonwoven air filters. Part II: Fiber diameter and crimp frequency. *Text Res J* 1979; 49: 79–87.
4. Song CB and Park HS. Analytic solutions for filtration of polydisperse aerosols in fibrous filter. *Powder Technol* 2006; 170: 64–70.
5. Steffens J and Coury JR. Collection efficiency of fiber filters operating on the removal of nano-sized aerosol particles: I-Homogeneous fibers. *Sep Purif Technol* 2007; 58: 99–105.
6. Lamb G and Costanza PA. Influences of fiber geometry on the performance of nonwoven air filters. *Text Res J* 1975; 45: 452–463.
7. Lamb G and Costanza PA. Influences of fiber geometry on the performance of nonwoven air filters: Part III: cross-sectional shape. *Text Res J* 1980; 50: 362–370.
8. Zhu C, Lin CH and Cheung CS. Inertial impaction-dominated fibrous filtration with rectangular or cylindrical fibers. *Powder Technol* 2000; 112: 149–162.
9. Ciach T and Gradon L. Multilayer fibrous filters with varied porosity and fiber diameter. *J Aerosol Sci* 1998; 29: 935–936.
10. Lisowski A, Jankowska E, Thorpe A, et al. Performance of textile fiber filter material measured with monodisperse and standard aerosols. *Powder Technol* 2001; 118: 149–159.
11. Heldmann C. Air filtration composite structures with superior filtration efficiency and optimised low pressure drop using finest meltblown and staple fibers. In: *proceedings of Filtrex08*, Köln, Germany, 2008.
12. Rupertseder W. Improved filter efficiency through integrated nanofibers. In: *proceedings of Filtrex08*, Köln, Germany, 2008.
13. Krucinska I. The influence of technological parameters on the filtration efficiency of electret needled non-woven fabrics. *J Electrost* 2002; 56: 143–153.
14. Zobel S, Maze B, Vahedi Tafreshi H, et al. Simulating permeability of 3-D calendered fibrous structures. *Chem Eng Sci* 2007; 62: 6285–6296.
15. Raynor PC and Leith D. The influence of accumulated liquid on fibrous filter performance. *J Aerosol Sci* 2000; 31: 19–34.
16. Contal P, Simao J, Thomas D, et al. Clogging of fiber filters by submicron droplets. Phenomena and influence of operating conditions. *Aerosol Sci* 2004; 35: 263–278.
17. Thomas D, Penicot P, Contal P, et al. Clogging of fibrous filter by solid aerosol particles: experimental and modelling study. *Chem Eng Sci* 2001; 56: 3549–3561.
18. Huang SH, Chen CW, Chang CP, et al. Penetration of 4.5 nm to 10 μm aerosol particles through fibrous filters. *Aerosol Sci* 2007; 38: 719–727.
19. Barrett LW and Rousseau AD. Aerosol loading performance of electret filter media. *Am Ind Hyg Assoc J* 1998; 59: 532–539.
20. Deeds WE. *Charging method for meltblown webs*. Patent number 5254297, USA, 1993.
21. Kim J, Jasper W and Hinestroza J. Direct probing of solvent-induced charge degradation in polypropylene electret fibres via electrostatic force microscopy. *J Microsc* 2007; 225: 72–79.
22. Smith PA, East GC, Brown RC, et al. Generation of triboelectric charge in textile fibre mixtures, and their use as air filters. *J Electrostat* 1988; 21: 81–98.
23. Kuwabara S. The forces experienced by randomly distributed parallel circular cylinders or spheres in a viscous

flow at small Reynolds numbers. *J Phys Soc Jpn* 1959; 14: 527–532.
24. Lee KW and Liu BYH. Theoretical study of aerosol filtration by fibrous filters. *Aerosol Sci Tec* 1982; 1: 147–161.
25. Davies CN. Filtration of aerosols. *J Aerosol Sci* 1983; 14: 147–161.
26. Thomas D, Contal P, Renaudin V, et al. Modeling pressure drop in HEPA filters during dynamic filtration. *J. Aerosol Sci* 1999; 30: 235–246.
27. Brown RC. *Air filtration*. London: Pergamon Press, 1993.
28. Frising T. *Etude de la filtration des aérosols liquides et de mélanges d'aérosols liquides et solides*. PhD Thesis, Institut National Polytechnique de Lorraine, France, 2004.
29. Liu BYH and Rubow KL. Efficiency, pressure drop and figure of merit of high efficiency fibrous and membrane filter media. In: *proceedings of 5th world filtration conference*, Nice, France, 1990.
30. Gougeon R. *Filtration des aérosols liquides par les filtres à fibers en régimes d'interception et d'inertie*. PhD Thesis, Université Paris XII, France, 1994.
31. Chen X, Vroman P, Lewandowski M, et al. Study of the influence of fiber morphology on liquid diffusion within nonwoven structures: effect of fiber diameter. *Text Res J* 2009; 79: 1364–1370.
32. Sakano T, Otani Y, Namiki N, et al. Particle collection of medium performance air filters consisting of binary fibers under dust loaded conditions. *Sep Purif Technol* 2000; 19: 145–152.
33. Brown RC and Thorpe A. Glass-fiber filters with bimodal fiber size distribution. *Powder Technol* 2001; 118: 3–9.
34. Jaganathan S, Vahedi Tafreshi H and Pourdeyhimi B. On the pressure drop prediction of filter media composed of fibers with bimodal diameter distribution. *Powder Technol* 2008; 181: 89–95.
35. Frising T, Thomas D, Contal P, et al. Influence of filter fiber size distribution on filter efficiency calculations. *Chem Eng Res Des* 2003; 81: 1179–1184.